

Evaluation of Direct Shear Tests on Geogrid Reinforced Soil

A.S.F.J. Sayão, A.C.C.F. Sieira

Abstract. This paper presents a program of direct shear tests in soil reinforced with geogrids, carried out with large-scale equipment. A woven geogrid was placed in sandy soil and positioned with different inclinations inside the shear box. The strength parameters of the soil-geogrid interface were obtained from shear tests with the geogrid positioned horizontally in the sand. The direct shear tests with inclined reinforcement revealed the strength differences related to the reinforcement inclination, seeking to define the most favorable positioning of the geogrid for construction works in reinforced slopes. An analysis of the deformed configuration of the geogrid is presented, based on the measured position of the grid at the end of the shear tests. Finally, numerical simulations of the direct shear tests were carried out, allowing an assessment of the tensile forces acting on the inclined reinforcement. These studies allowed a clear definition of the soil region that is not distorted during the direct shear test, being subject to a simple translation only. The geogrid's displacements were found to be anti-symmetrical in relation to the failure plane. Shearing was concentrated at the central region of the specimen's height, with the upper and lower regions being simply subjected to translation, with no distortion. The inclination of the reinforcement within the soil has a significant influence, with the maximum strength occurring when the geogrid was positioned at 60° angle in relation to the failure plane.

Keywords: reinforced soil, geogrids, direct shear tests, numerical analyses.

1. Introduction

Geogrids are flat synthetic structures consisting of fully connected traction resistant elements in the form of a grid. In addition to the surface available for interface friction between the grid elements and the soil, geogrids also have a hollow area for the mobilization of soil-soil shear strength.

The interaction mechanism developed in the soil-geogrid interface depends on the physical and mechanical characteristics of the soil and the geogrid. A reinforced soil structure project requires knowledge of the interface strength parameters, which can be obtained from pullout, direct shear or inclined plane tests.

These test methods have basic differences in the boundary conditions, stress paths and failure mechanisms imposed to the specimen. The choice of one of these tests must take into account the similarity with the load conditions found in reinforced soil construction works. (Palmeira & Milligan, 1989). A comprehensive review on the advantages and limitations of these tests is presented by Palmeira (2009).

The direct shear tests herein described are aimed at the reproduction of two distinct mechanisms of interaction that occur in the soil-geogrid interface. The first involves the mobilization of interface friction, whereas its reproduction in the laboratory allows the strength parameters of the soil-geogrid interface to be obtained. The second mechanism consists of the mobilization of tensile loads in the

geogrid. Figure 1 illustrates the two different interaction mechanisms in geosynthetic reinforced soil.

In the first mechanism, the geogrid remains attached to the lower part of the enveloping soil, with the interface resistance being mobilized by the sliding of the upper soil mass in relation to the geogrid. In this case, the interface strength parameters ($\phi'_{s/GGR}$ and $c_{s/GGR}$) can be obtained from direct shear tests with the geogrid horizontally positioned in the test box.

Interface shear has been studied by several researchers. Bakeer *et al.* (1998) discussed the strength parameters obtained from direct shear and pullout tests for an aggregate-geogrid interface. Wasti & Ozdugun (2001) compared results of horizontal reinforcement in direct shear tests to results of inclined plane tests (or tilt tests). Lui *et al.* (2009) reported on the results of shear tests with different soil-geogrid interfaces. Pitanga *et al.* (2009) studied the interface shear strength in inclined plane tests on from landfill cover materials. Slightly higher interface parameters have usually been found when obtained from direct shear tests with horizontal reinforcement as compared to inclined plane tests.

The second interaction mechanism occurs when the potential failure surface intercepts the geogrid. A laboratory simulation can be achieved in direct shear tests of soil specimens with reinforcement inclined in relation to the horizontal shear surface. The maximum tension of the geogrid occurs at the point where it is intercepted by the failure surface. In this mechanism, shear stresses on the soil-

A.S.F.J. Sayão, Associate Professor, Departamento de Engenharia Civil, Pontifícia Universidade Católica do Rio de Janeiro, Rio de Janeiro, RJ, Brazil. e-mail: sayao@puc-rio.br.

A.C.C.F. Sieira, Associate Professor, Departamento de Estruturas e Fundações, Universidade do Estado do Rio de Janeiro, Rio de Janeiro, RJ, Brazil. e-mail: sieira@uerj.br.
Submitted on December 2, 2010; Final Acceptance on April 3, 2012; Discussion open until September 30, 2012.

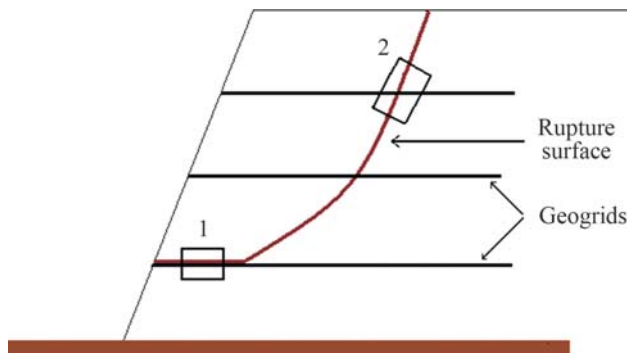


Figure 1 - Soil-geogrid interaction mechanisms: (1) interface shear; (2) tension in reinforcement.

geogrid interface are absorbed by the tensioned reinforcement.

Figure 2 illustrates the direct shear test with an inclined reinforcement. The geogrid's function in a reinforced slope consists of overcoming the soil's incapacity to resist tensile stresses. When the failure surface intercepts the geogrid, this becomes tensioned, thereby giving the reinforced soil mass a stabilizing effect. The angle θ , between the reinforcement and the failure surface, has a significant influence on the soil-geogrid resistance and changes from its initial value θ_0 to a final value θ_f at the end of the shearing. This variation in θ will depend on the magnitude of angular distortions and on the thickness of the shear zone, as illustrated in Fig. 3.

Bauer & Zhao (1994) presented results of direct shear tests with inclined reinforcement, using uniform sand and a polypropylene geogrid. Inclination angle θ was shown to have a large influence on the soil-geogrid resistance. When compared to the non-reinforced soil, the maximum increase in strength occurred when the geogrid was positioned at $\theta_0 = 60^\circ$ in relation to the failure plane.

Sayão & Teixeira (1995) carried out direct shear tests with an inclined unwoven geotextile for simulating the field condition of an embankment over soft clay. In these

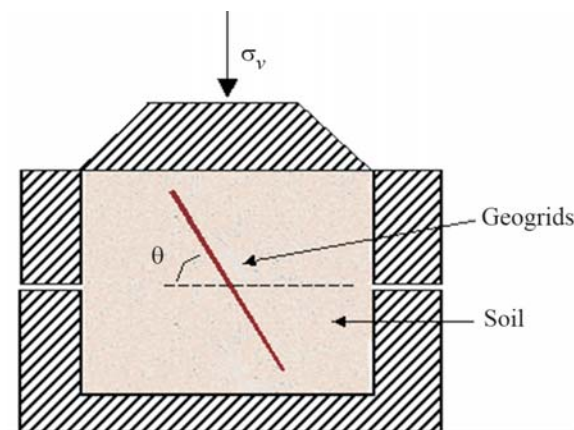


Figure 2 - Direct shear tests with inclined reinforcement.

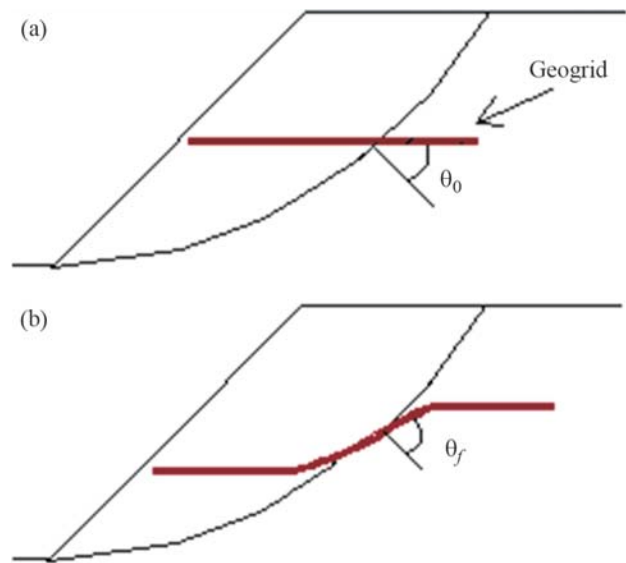


Figure 3 - Reinforcement behavior in a shear zone. (a) initial condition; (b) distorted condition.

tests, the reinforcement was positioned at an inclined angle within the layered soil specimens, which were made of clay in the lower half and sand in the upper half. The shear strength parameters of the soil-geotextile interface were noted to vary with the geotextile inclination θ , but further research on larger devices was suggested.

Palmeira (1999) also concluded that the most favorable orientation of the reinforcement element in large-size shear tests was 60° , because it coincided with the direction of the tensile strain increments of the unreinforced soil.

The main objective of this investigation was to obtain a clear definition of the soil region that is distorted during the direct shear test. This was achieved with shear tests with inclined reinforcement, in which the grid's displacements were measured for defining its deformed shape. The observations were complemented by numerical simulations of the direct shear tests.

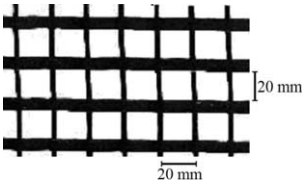
2. Materials

All tests were carried out with a geogrid reinforced sandy soil in large-scale direct shear apparatus at the Cedex geotechnical laboratory, in Spain.

2.1. Geogrid characteristics

The geogrid exhibits a 20 mm opening size and 70% of open area available for the mobilization of soil-soil friction during direct shearing. According to the manufacturer, this geogrid is bi-axially oriented, with woven fibers of high-tenacity polyester and low tendency to creep. The polyester filaments are coated with PVC for protecting the nucleus against damage during installation and working procedures. Nominal values for longitudinal and transversal tensile strengths are 97.0 kN/m and 29.4 kN/m, respectively. Table 1 shows the main physical and mechan-

Table 1 - Physical and mechanical characteristics of geogrid.

Physical		
	Type of polymer	Polyester with PVC
	Manufacturing process	Woven
	Type of mesh	Square openings
	Openings of grid	20.0 mm
	Width of longitudinal elements	8.0 mm
	Width of transversal elements	3.0 mm
Mechanical	Longitudinal tensile strength	97.0 kN/m
	Transverse tensile strength	29.4 kN/m
	Tensile elongation at failure	12.8%
	Longitudinal stiffness	750.0 kN/m

ical characteristics of geogrid used in the experimental program.

2.2. Sandy soil characteristics

The sand used in the experimental program consisted predominantly of quartz and feldspar and contained particles with a specific gravity $G_s = 2.71$ and average diameter $D_{50} = 0.7$ mm.

All sand specimens were compacted in the laboratory to a relative density $D_r = 80\%$, with water content $w = 10 \pm 0.2\%$, corresponding to a saturation degree $S = 37\%$. These values are typical for sandy embankments in reinforcement projects. Shear strength parameters of the sand were $c' = 16$ kPa (cohesion) and $\phi' = 33^\circ$ (friction angle). These parameters were obtained in the large size direct shear device under vertical confining stresses of 50, 100 and 200 kPa, for avoiding errors due to scale effects in the interpretation of reinforced test results.

3. Experimental Program

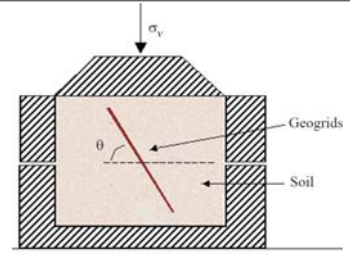
3.1. Direct shear tests

The experimental program consisted of twelve direct shear tests with the geogrid positioned at different inclinations inside the soil specimen, as shown in Table 2. Vertical confining stresses of 50, 100 and 200 kPa were imposed to each specimen configuration.

Direct shear tests with the horizontal geogrid ($\theta = 0^\circ$) aimed at the simulation of interaction mechanism no. 1, as

Table 2 - Direct shear tests program in reinforced soil.

Vertical confining stress, σ_v (kPa)	Inclination of geogrid, θ
50, 100 and 200	0°
	30°
	60°
	90°



shown in Fig. 1, for obtaining the soil-geogrid interface parameters (interface friction angle, $\phi'_{s/GSY}$, and soil-geogrid adhesion, $c_{s/GSY}$). The shear tests with inclined reinforcement ($\theta = 30^\circ$, 60° and 90°) aimed at reproducing mechanism no. 2 and obtaining the shear strength variation as a function of the reinforcement inclination.

3.2. Equipment

Figure 4 shows the large size direct shear device used in the experimental program. The equipment used was originally developed in the Cedex Laboratory (Spain) to study the shear resistance of rockfill materials (Sayão *et al.*, 2005) and adapted to direct shear and pullout tests on soil specimens containing geosynthetic materials (Sieira & Sayão 2006, and Sieira *et al.* 2009).

The shear box is made of aluminum and divided into two halves with a square section with 1.0 m sides and a height of at least 0.70 m. The device is composed of two systems for vertical and horizontal load application. Each system consists of a hydraulic jack, a servo-control, a load cell and a displacement transducer.

The vertical hydraulic jack has a load capacity corresponding to a confining stress of 1.0 MPa. The vertical servo-control ensures the steadiness of σ_v during the test. The load signal applied to the test specimen is continually compared to the reference signal, which corresponds to the desired normal stress. Upon any difference between the two signals, the servo-control switches on the hydraulic jack to correct the applied vertical load. Increases in σ_v , produced by reductions in the contact area between the lower and upper halves of the shear box, can therefore be compensated.

The horizontal load system functions in a similar way. The horizontal servo-control guarantees a constant average shear strain rate during the test. The maximum elongation of the horizontal hydraulic jack piston is 300 mm. This was sufficient to produce a shear failure in all specimens tested in this experimental program.

3.3. Test procedure

Testing in the large size shear device is similar to the conventional direct shear tests: the upper half of the box remains immobile, while the lower half is displaced by the

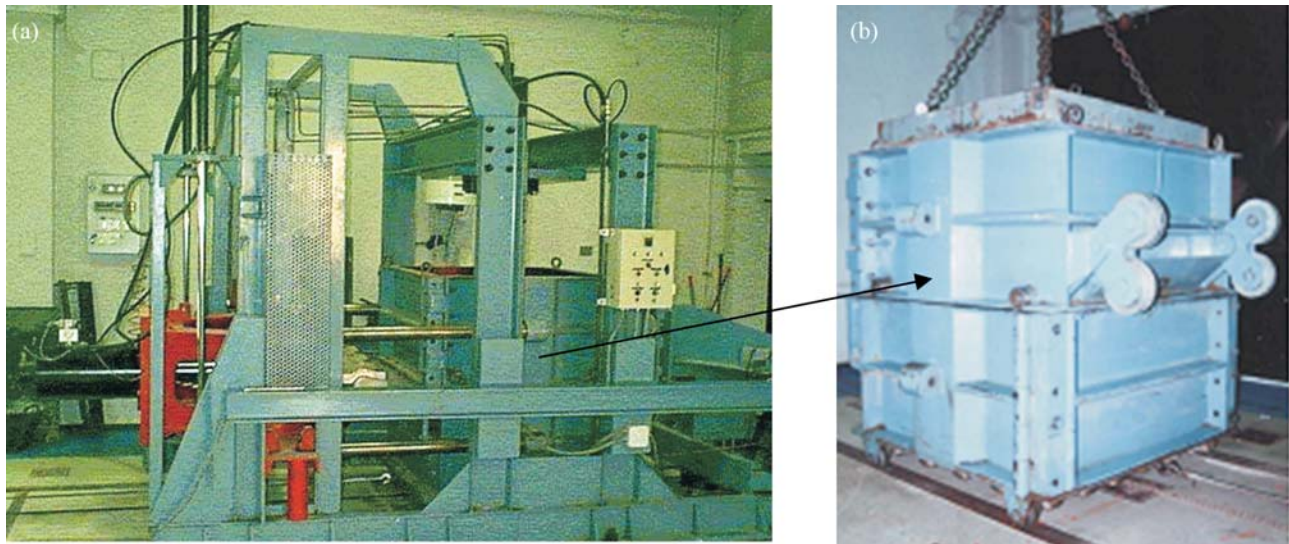


Figure 4 - Large-scale direct shear test equipment. (a) lateral view; (b) detail of shear box.

horizontal hydraulic jack. More details about this equipment are given in Sieira & Sayão (2006).

Direct shear tests with inclined reinforcement were carried out with a dense silty sand ($D_r = 80\%$), compacted in four successive layers. To achieve the prescribed relative density, the quantity of soil needed to fill a layer was statically compacted using the vertical jack until the required height was reached.

In direct shear with inclined reinforcement, the tests box was first totally filled with soil, and then the specimen was cut at the desired inclination and the soil removed was carefully kept separated. The geogrid was subsequently placed in position (Fig. 5) and the sand was placed for back filling the rest of the test box at the desired density.

After the specimen preparation, the top cap was put in position and the box placed inside the equipment. The hydraulic jacks were adjusted and the direct shear test was then started. Vertical confining stresses of 50, 100 and 200 kPa were applied during the direct shear tests, including the overload imposed by the cap weight.

3.4. Measurement of the internal displacement of the geogrid

The inner displacements and distortions of the geogrid in the shear box were evaluated at the end of the tests. Figure 6 schematically shows the geogrid configuration before and after a test with vertical reinforcement. Points A, B and C represent the positions of the vertical geogrid at the beginning of the shear test, while points A', B' and C' represent the deformed configuration of the geogrid upon completion.

This deformed configuration was obtained after careful dismantling of the soil specimen. The final positioning of different points of the geogrid was recorded in the test box. This final configuration of the distorted geogrid allows

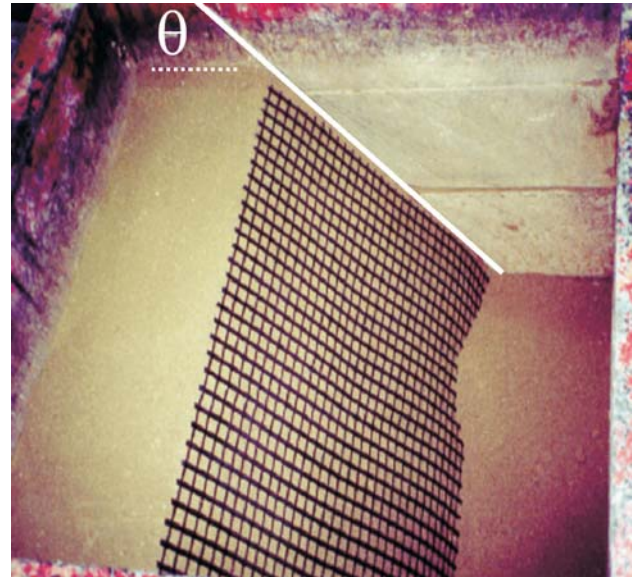


Figure 5 - Upper view of the geogrid after positioning at $\theta = 60^\circ$ in the shear box.

identification of three regions within the direct shear specimen: the central zone, where the shearing occurs, and the upper and lower external zones, where the soil is subject to a simple translation with no distortion.

4. Numerical Simulation of Tests with Inclined Reinforcement

The objective of the numerical simulations consisted in the visualization of mobilized stresses and strains in the geogrid at the end of the direct shear tests.

The first direct shear test simulation was done with non-reinforced sand. After the stress-strain parameters of

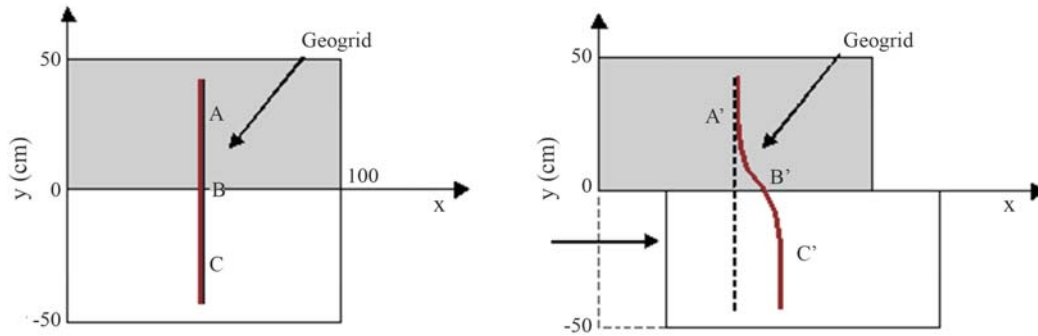


Figure 6 - Configuration of the geogrid in the test box before and after shearing. (a) initial condition; (b) end of test.

the sand were correctly defined, the geogrid was introduced with the proper inclination in relation to the failure plane.

4.1. Computer program

All simulations made use of the Plaxis computer program (Brinkgreve & Vermeer, 1998). The soil mass is divided in finite elements obeying pre-defined stress-strain relations and the reinforcement element requires only the axial stiffness as input parameter.

The use of a bi-dimensional program to represent the tri-dimensional geogrid may impose a restriction, as the mobilized passive resistance at transversal strips cannot be taken into account. However, in direct shear tests with inclined reinforcement, geogrids are basically subjected to tensile loading and the simulations with a 2D program are acceptable.

The direct shear tests were simulated by a finite element mesh with proper boundary conditions. Vertical confinement was simulated through a uniform load on the top horizontal boundary, which was free to move vertically. The shearing phase was then imposed by increasing the horizontal load on the vertical wall of the lower box, which was free to move horizontally. During this phase, all elements in the upper box could only move vertically.

4.2. Stress-strain model

To represent the stress-strain behavior of the sand, a perfectly plastic model was adopted, using the Mohr-Coulomb failure criteria. This model requires the definition of five simple soil parameters: Young's modulus (E), Poisson's ratio (ν), specific weight (γ), effective cohesion (c') and effective friction angle (ϕ').

Table 3 shows the parameters obtained for non-reinforced sand, as a function of the vertical stress, from large

Table 3 - Geotechnical parameters of the sand.

σ'_v (kPa)	c' (kPa)	ϕ' (°)	E (MPa)	ν
50	16	33	3.5	0.3
100	16	33	8.0	0.3
200	16	33	17.0	0.3

size direct shear tests. Deformability parameters were determined numerically after adequately reproducing the shear test results, as indicated in Fig. 7.

For the analyses of tests with inclined reinforcement, the geogrid stiffness (750 kN/m) was determined from the unconfined tensile test results provided by the manufacturer.

The geogrid was introduced into the numerical analyses with different inclinations (0° , 30° , 60° and 90°) in relation to the failure plane. Irrespective of the inclination, boundary effects were avoided by positioning the geogrids 50 mm distant from the upper and lower borders.

Soil-geogrid interaction is modeled by interface elements. The type and magnitude of interaction are defined by an adequate value for the interface strength reduction factor (R_{inter}). This factor may be defined as the ratio between the interface strength and the soil strength, as given by the equation:

$$R_{inter} = \frac{\tan \phi_{s/GGR}}{\tan \phi'} \quad (1)$$

where $\phi_{s/GGR}$ = interface friction angle; ϕ' = soil's friction angle.

In this investigation, a value of $R_{inter} = 0.92$ was adopted based on results of direct shear tests with horizon-

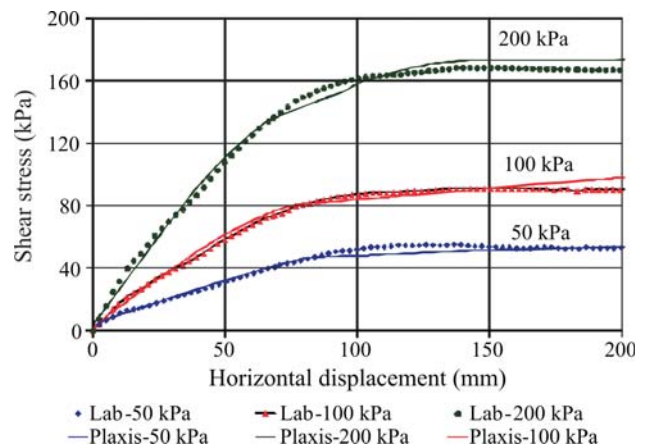


Figure 7 - Numerical reproduction of direct shear tests in sand specimens.

tal reinforcement. These tests designate the shear strength at the soil-geogrid interface, as presented in the next section.

5. Experimental Results

5.1. Shear strength

Results from direct shear tests are shown in Fig. 8 and corresponding strength parameters are presented in Table 4. In tests with inclined reinforcement ($\theta > 0$), shearing does not occur on the soil-geogrid interface. Accordingly, the parameters $c_{s/GGR}$ and $\phi_{s/GGR}$ listed in Table 4 do not represent soil-geogrid interface adhesion and friction. They express the strength of the reinforced soil mass arising from the mobilization of tensile stresses in the geogrid.

Specimens with horizontal reinforcement ($\theta = 0^\circ$) resulted in soil-geogrid parameters of $c_{s/GGR} = 15.7$ kPa (adhesion) and $\phi_{s/GGR} = 34.6^\circ$ (friction angle). These interface values were slightly lower than the strength parameters (c' and ϕ') for the sandy soil, providing the following interaction coefficients:

$$\lambda_{s/GGR} = \frac{c_{s/GGR}}{c'} \quad (2)$$

$$f_{s/GGR} = \frac{\tan \phi_{s/GGR}}{\tan \phi} \quad (3)$$

Figure 9 shows the variation in shear resistance due to the reinforcement inclination for three levels of vertical

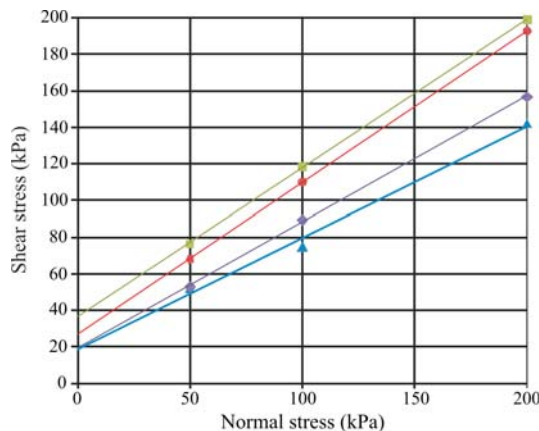


Figure 8 - Direct shear test results in reinforced sand specimens with inclined geogrid.

Table 4 - Strength parameters from direct shear tests.

θ ($^\circ$)	$c_{s/GGR}$ (kPa)	$\phi_{s/GGR}$ ($^\circ$)
0	15.7	34.6
30	26.8	36.0
60	36.2	39.1
90	19.2	35.0

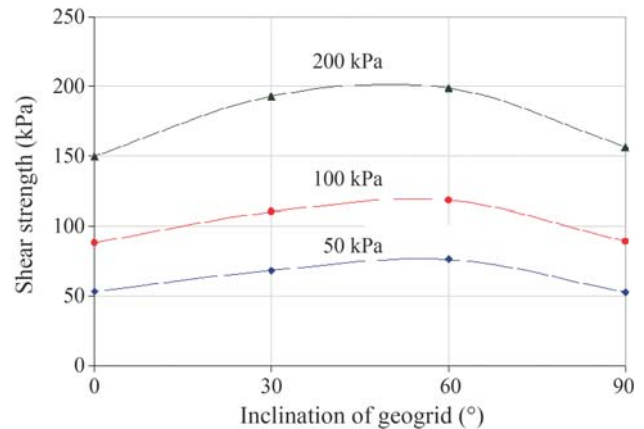


Figure 9 - Variation of shear strength as a function of geogrid inclination.

confining stress (50, 100 and 200 kPa). The maximum variation corresponds to the optimal inclination of the geogrid (about 55° to 60° in Fig. 9). This conclusion may be in accordance with the classical Rankine's theory, which predicts for vertical slopes a potential failure surface inclined by $45^\circ + \phi'/2$ with the horizontal. For the sandy soil considered herein ($\phi' = 37^\circ$), the theoretical optimum inclination of the reinforcement layer will then be $\theta = 63^\circ$. This is not far from the range of optimum geogrid inclinations (about 55 to 60°) indicated in Fig. 9.

These results therefore suggest that, in reinforced soil, geogrid layers shall be placed at the horizontal direction. This will impose an angle of approximately 60° between the geogrid and the potential failure surface, resulting in maximum shear resistance mobilization.

Conclusions supporting that $\theta = 60^\circ$ is the most favorable geogrid inclination relative to the shear surface were also reported by Jewell & Wroth (1987) and Palmeira (1999).

5.2. Distortion of geogrid during shearing

Figure 10 illustrates the initial and final positions of the geogrid for tests with different levels of vertical stress (σ_v) and different inclinations (θ) of reinforcement in relation to the failure surface. This figure illustrates only the upper half of the test box (the shaded half in Fig. 5). The displacements in the lower half of the shear box may be considered to be anti-symmetrical in relation to the upper box. It should be emphasized that the magnitudes of the horizontal displacement (dh) indicated in Fig. 10 corresponds to the total displacement between the two halves at the end of shearing.

It can be noted that the shearing is concentrated in the central region, corresponding to approximately 35% of the box height. Outside this (*i.e.*, in the top and bottom regions, corresponding to the remaining 65% of the specimen), there is practically no distortion taking place in the soil or in the geogrid. In these external regions, dislocation of the

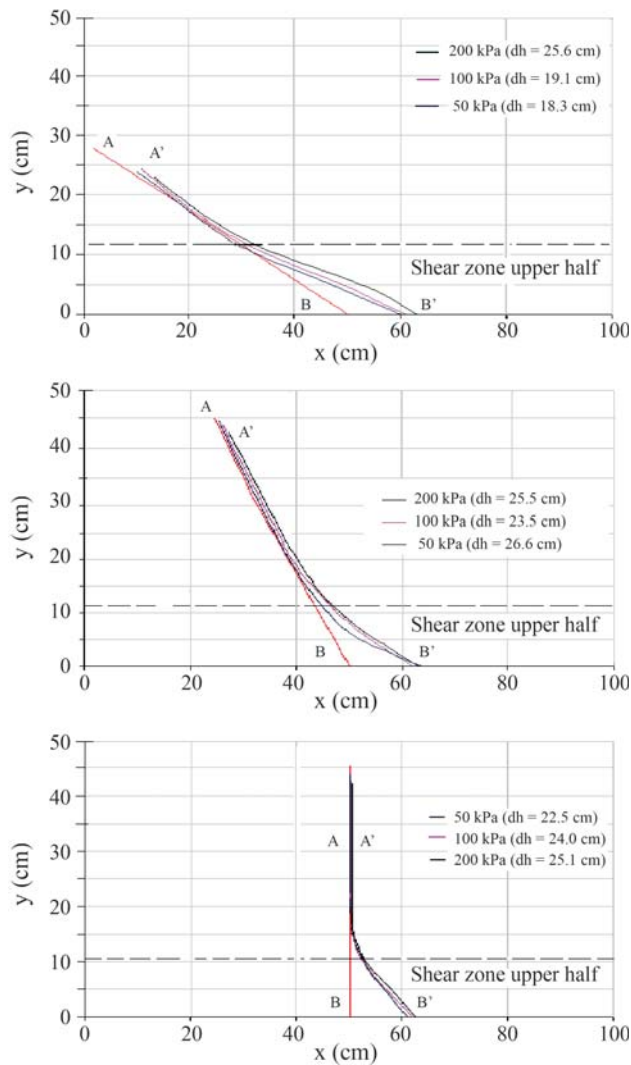


Figure 10 - Final positions of geogrids in the upper half of direct shear box. (a) Geogrid at $\theta = 30^\circ$; (b) Geogrid at $\theta = 60^\circ$; (c) Geogrid at $\theta = 90^\circ$.

rigid box induces a simple translation of the geogrid mesh. This conclusion indicates that a small variation in the height of the box would not interfere with the results, since the volume subject to shearing is restricted to the internal part of the specimen.

It can also be noted that the geogrid's final displacements in the shearing zone increase slightly with the vertical confining stress. This may be clearly noted in Fig. 11. In fact, an increase in σ_v corresponds to an increase in shear stress and therefore to greater geogrid distortions at the end of the test. Consequently, greater tensile stresses in the geogrid are expected for higher levels of normal stress σ_v .

6. Numerical Analysis

Figure 12 shows the numerical predictions of the shear test results with the geogrid installed vertically in the soil specimen. The predicted curves do not exhibit a peak or

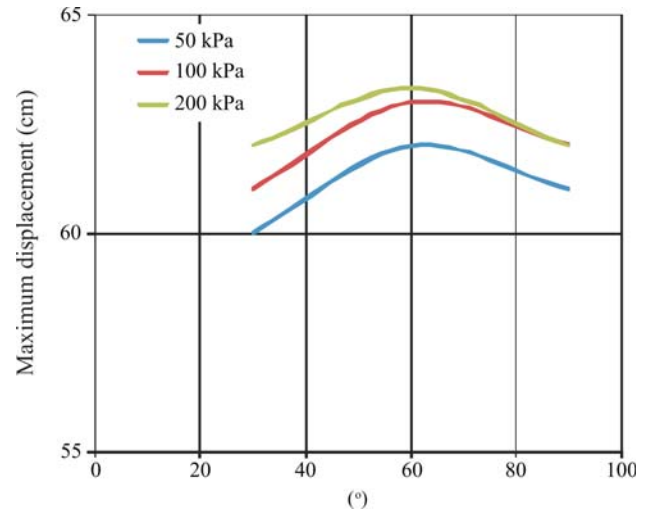


Figure 11 - Final displacement of geogrid in the shearing surface as a function of inclination angle and confining stress.

a stabilization strength level. This behavior was observed in all simulations of the direct shear tests and is strictly related to the loading mechanism. After large displacements, the lower box tends to make contact with the upper box, imposing an additional constraint to the relative movement between the two boxes. For displacements smaller than 100, however, this restriction is negligible.

Figure 13 shows the deformed geogrid configuration, as predicted by the numerical analysis at the end of the $\theta = 90^\circ$ tests with a confinement level of 200 kPa. It can be seen that the displacements are anti-symmetrical in relation to the failure plane. The predicted distortions of the geogrid are similar to what was observed in the laboratory. The shear zone, which may be defined as the region where the

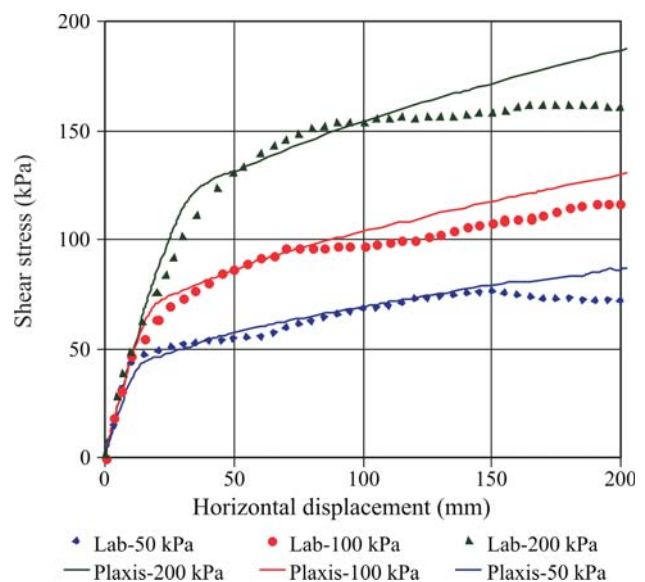


Figure 12 - Reproduction of the direct shear tests with geogrid at $\theta = 90^\circ$.

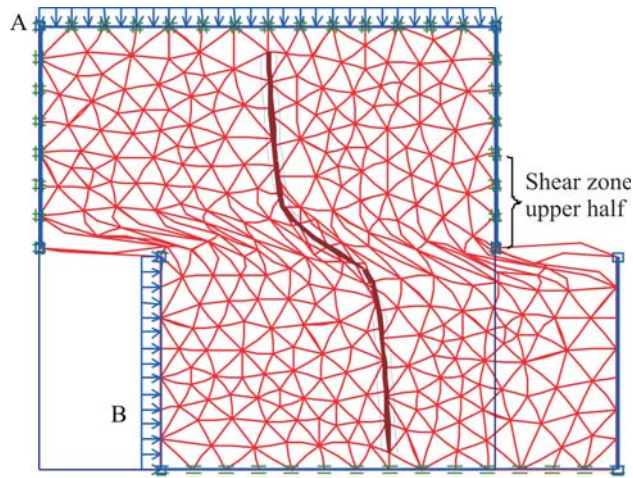


Figure 13 - Deformed configuration of geogrid at inclination $\theta = 90^\circ$.

geogrid distortion occurs, corresponds to no more than 33% of the shear box height, as shown in the analysis of the experimental results.

The measured horizontal displacements were compared with those estimated through the numerical simulation. Figure 14 shows the upper right quadrant of the shear box with the final positions of the geogrid. Adequate agreement of the results can be observed, suggesting that the numerical analysis is capable of satisfactorily reproducing the laboratory tests.

Figure 15 shows the deformed configuration of the geogrid, predicted at the end of the tests with $\theta = 60^\circ$ and $\sigma'_v = 100$ kPa. The relative displacement between the upper and the lower boxes was 243 mm. An anti-symmetric shape in relation to the failure plane is to be noted at the distorted geogrid. At the geogrid's extremities there was no distortion in the finite element mesh, indicating that these regions were not affected by shearing. Once again the shear zone corresponds to the central third of the total box height.

Figure 16 shows the points of the soil mass that reached the yield or failure condition in direct shear test simulations with the geogrid inclined at $\theta = 30$ and 60° .

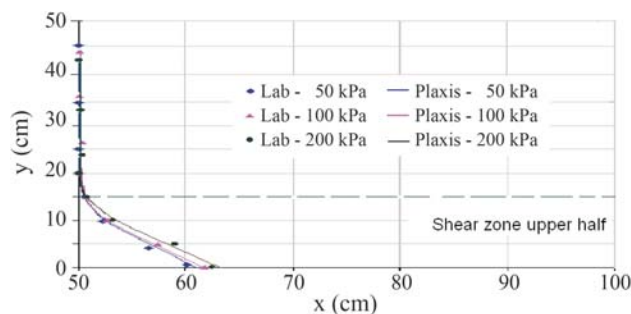


Figure 14 - Predicted and measured displaced positions of geogrid at inclination $\theta = 90^\circ$.

These yielded points are observed to be confined to the specimen's central zone, which is away from the upper and lower undistorted regions of the soil within the shear box.

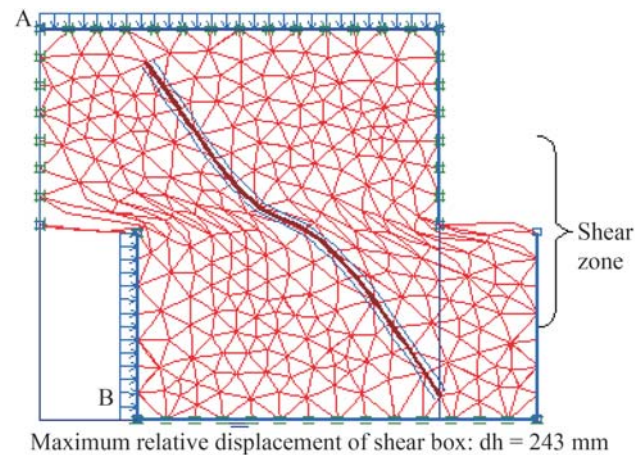


Figure 15 - Deformed configuration of the geogrid at inclination $\theta = 60^\circ$.

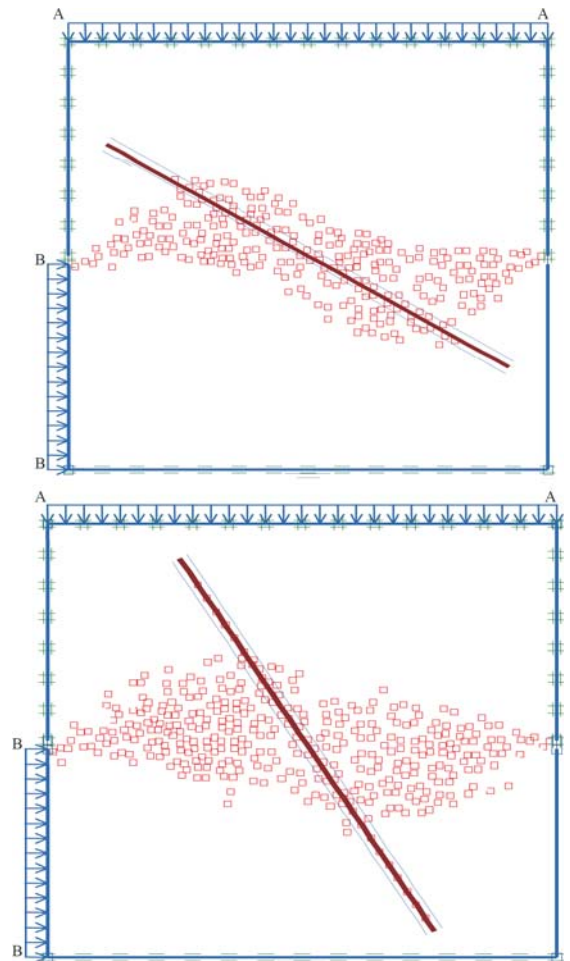


Figure 16 - Soil elements that reached a yielding state in shear tests with inclined geogrid. (a) Geogrid at inclination $\theta = 30^\circ$; (b) Geogrid at inclination $\theta = 60^\circ$.

Similar results were obtained from simulations with geogrid at other inclinations.

The numerical strain analysis, as well as the measurements of the geogrid displacements, indicates that the height of the direct shear box may be reduced without affecting the test results. The identification of the distorted region is particularly relevant in large scale tests, as it can allow a substantial reduction of the specimen volume to be used. In the case of the tests reported herein, this reduction can larger than 0.5 m^3 , which would be equivalent to at least 800 kg of compacted soil, with a relevant saving in time preparation of the soil specimen.

The tensile stresses in the geogrid at the end of the direct shear tests are shown in Fig. 17, for the three levels of vertical confining stress. The maximum tension value (T_{\max}) occurs in the central region of the geogrid, which is the region most demanded during shearing. Furthermore, the tensile stress tends to be annulled at the geogrid's extremities.

Higher levels of normal stress indicate higher tensile stress in the geogrid, as shown in Fig. 18. As the highest tensile stress was estimated to be 48 kN/m, in the test with the geogrid inclined at $\theta = 60^\circ$, maximum mobilization of the geogrid corresponded to about 50% of the maximum tensile strength of 97 kN/m.

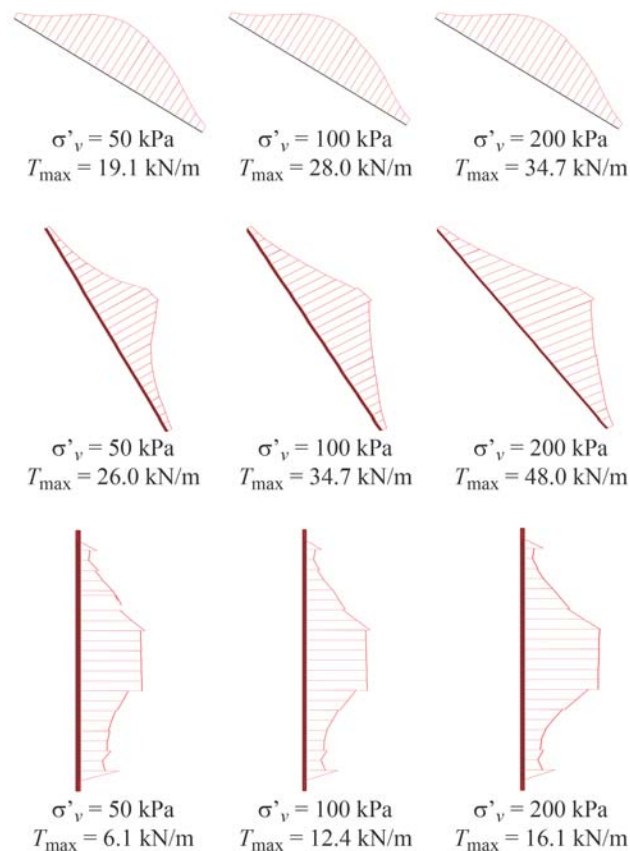


Figure 17 - Tensile stresses along the geogrid at different inclinations to the failure plane. (a) $\theta = 30^\circ$; (b) $\theta = 60^\circ$; (c) $\theta = 90^\circ$.

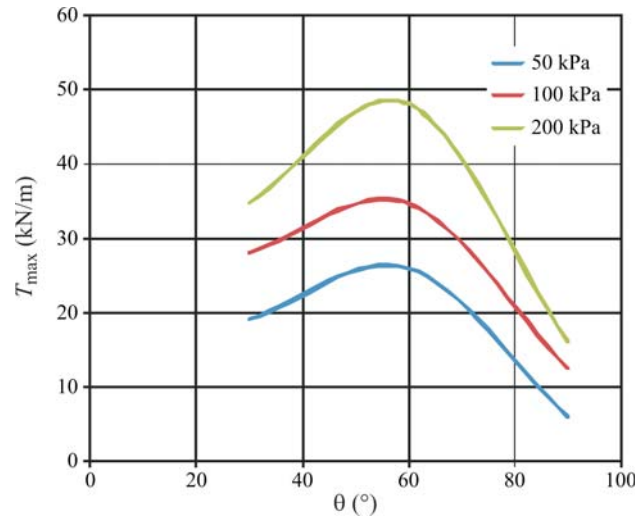


Figure 18 - Variation of maximum tensile stress as a function of geogrid inclination and confinement.

7. Conclusions

This paper presents the results of a direct shear test program with inclined geogrids reinforcing the soil specimens. The tests were carried out using a large-scale device and the reinforcement was positioned with different inclinations within the shear box.

Numerical simulations using a finite element program were carried out with the aim of determining the deformed geogrid configuration and the tensile stresses in the geogrid.

The numerical and experimental results indicated that the geogrid's displacements were anti-symmetrical in relation to the failure plane. For the 1 m high soil specimen, shearing was concentrated approximately at the central one third of the specimen's height. The upper and lower regions of the specimen were simply subjected to translation, with no distortion taking place due to displacement of the shear box. This verification suggests that the large-scale direct shear tests may be carried out in equipment with a lower height, with a considerable reduction of the soil volume to be used in preparing the test specimens.

The analysis of stresses in the geogrid at the end of the tests indicated that the maximum tension value (T_{\max}) occurs in the central region of the geogrid, which is the region most demanded during shearing. A similar behavior for the three inclinations of geogrid in the box test was observed. The increase in confining stress test induces higher tensile stresses in the geogrid. The maximum tensile stress was predicted to be 48 kN/m, in the test with the geogrid inclined at $\theta = 60^\circ$. This value corresponds to around 50% of the reinforcement's peak strength.

The geogrid inclination in relation to the failure plane has a significant influence on the soil-geogrid resistance. The maximum increase in strength occurred when the geo-

grid was positioned at an angle of $\theta = 60^\circ$ in relation to the failure plane. This is the most favorable geogrid inclination relative to the potential shear surface in reinforced soil projects.

Acknowledgments

The research described herein was funded by the National Research Council of Brazil (CNPq). The authors are indebted to Maccaferri Brazil for supporting the research on geogrids, and to the Geotechnical Laboratory at Cedex (Spain) for the availability of experimental facilities.

References

- Bakeer, R.M.; Sayed, S.M.; Cates, P. & Subramanian, R. (1998) Pullout and shear tests on geogrid reinforced lightweight aggregate. *Geotextiles and Geomembranes*, v. 16:2, p. 119-133.
- Bauer, G.E. & Zhao, Y. (1994) A realistic stress transfer model for geogrids in pullout. *Proc. 5th International Conference on Geotextiles, Geomembranes and Related Products*, Singapore, pp. 457-460.
- Brinkgreve, R.B.J. & Vermeer, P.A. (1998) *Plaxis, Finite Element Code for Soil and Rock Analyses*. Balkema, Rotterdam, Netherlands, 614 pp.
- Jewell, R.A., Wroth, C.P. (1987) Direct shear test on reinforced sand. *Geotechnique*, v. 37:1, p. 53-68.
- Lui, C.N.; Ho, Y.H. & Huang, J.W. (2009) Large scale direct shear tests of soil / PET-yarn geogrid interfaces. *Geotextiles and Geomembranes*, v. 27:1, p. 19-30.
- Palmeira, E.M. (1999) Execution and interpretation of laboratory tests on geosynthetic material (in Portuguese). *Proc. 1st South-American Symposium on Geosynthetics, ABMS-ISSMGE*, Rio de Janeiro, Brazil, v. 1, pp. 87-108.
- Palmeira, E.M. (2009) Soil-geosynthetic interaction: Modelling and analysis. *Geotextiles and Geomembranes*, v. 27:5, p. 368-390.
- Palmeira, E.M. & Milligan, G.W.E. (1989) Large scale direct shear tests on reinforced sand. *Journal Soils and Foundations (Japan)*, v. 29:1, p. 18-30.
- Pitanga, H.N.; Gourc, J.P. & Vilar, O.M. (2009) Interface shear strength of geosynthetics: evaluation and analysis of inclined plane tests. *Geotextiles and Geomembranes*, v. 27:6, p. 435-446.
- Sayão, A.S.F.J. & Teixeira, M.L. (1995) Use of geosynthetics for reinforcement of earthfills over soft soils (in Portuguese). *Proc. 2nd Brazilian Symposium on Applications of Geosynthetics, ABMS*, São Paulo, Brazil, pp. 169-180.
- Sayão, A.S.F.J.; Maia, P.C.A. & Nunes, A.L.L.S. (2005) Considerations on the shear strength behavior of weathered rockfill. *Proc. 16th International Conference on Soil Mechanics and Geotechnical Engineering, ISSMGE*, Osaka, Japan, v. 3, Section 2f, pp. 1917-1920.
- Sieira, A.C.C.F. & Sayão, A.S.F.J. (2006) Pullout tests on mechanically damaged geogrids (in Spanish). *Revista Ingeniería Civil*, n. 141, pp. 63-72.
- Sieira, A.C.C.F.; Gerscovich, D.M.S. & Sayão, A.S.F.J. (2009) Displacement and load transfer mechanisms of geogrids under pullout conditions. *Geotextiles and Geomembranes*, v. 27, n. 4, p. 241-253.
- Wasti, Y. & Ozdüzgun, Z.B. (2001) Geomembrane-geotextile interface shear properties as determined by inclined board and direct shear box tests. *Geotextiles and Geomembranes*, v. 19:1, p. 45-57.

List of Symbols

- c' = effective cohesion of soil
 $c_{s/GGR}$ = soil-geogrid adhesion parameter
 $c_{s/GSY}$ = soil-geosynthetic adhesion parameter
 D_{50} = average diameter of soil particles
 D_r = relative density of soil
 E = Young's modulus
 $f_{s/GGR}$ = soil-geogrid interaction coefficient
 G_s = specific gravity of soil particles
 R_{inter} = interface strength reduction factor
 S = saturation degree of soil
 T_{max} = maximum tensile load
 w = water content of soil
 ϕ' = effective friction angle of soil
 $\phi'_{s/GGR}$ = effective soil-geogrid interface friction angle
 $\phi'_{s/GSY}$ = effective soil-geosynthetic interface friction angle
 γ = specific weight of soil
 ν = Poisson's ratio
 θ = inclination of geogrid in relation to failure surface
 σ_v = vertical confining stress
 τ = shear stress